NANO LETTERS

Letter

pubs.acs.org/NanoLett

Crystalline Liquid and Rubber-Like Behavior in Cu Nanowires

Yonghai Yue,[†,¶] Nianke Chen,[‡] Xianbin Li,[‡] Shengbai Zhang,[*,‡,§] Ze Zhang,[*,†,∥] Mingwei Chen,[⊥] and Xiaodong Han[*,†]

[†]Institute of Microstructure and Properties of Advanced Materials, Beijing University of Technology, Beijing, 100124, China

[‡]State Key Laboratory on Integrated Optoelectronics College of Electronic Science and Engineering, Jilin University, Changchun 130012, China

[§]Department of Physics, Applied Physics, and Astronomy, Rensselaer Polytechnic Institute, Troy, New York 12180, United States

[∥]Department of Materials Science, State Key Lab of Si Materials, ZheJiang University, Hangzhou, Zhejiang, 310058, China

[⊥]WPI Advanced Institute for Materials Research, Tohoku University, Sendai 980-8577, Japan

[¶]School of Chemistry and Environment, Beihang University, Beijing, 100191, China

S *Supporting Information*

ABSTRACT: Via in situ TEM tensile tests on single crystalline copper nanowires with an advanced tensile device, we report here a crystalline-liquid-rubber-like (CRYS-LIQUE-R) behavior in fracturing crystalline metallic nanowires. A retractable strain of the fractured crystalline Cu nanowires can approach over 35%. This astonishing CRYS-LIQUE-R behavior of the fracturing highly strained single crystalline Cu nanowires originates from an instant release of the stored ultralarge elastic energy in the crystalline nanowires. The release of the ultralarge elastic energy was estimated to generate a huge reverse stress as high as ~10 GPa. The effective diffusion coefficient (D_{eff}) increased sharply due to the consequent pressure gradient. In addition, due to the release of ultrahigh elastic energy, the estimated concomitant temperature increase was estimated as high as 0.6 Tm (Tm is the melting point of nanocrystalline Cu) on the fractured tip of the nanowires. These factors greatly enhanced the atomic diffusion process. Molecular dynamic simulations revealed that the very high reverse stress triggered dislocation nucleation and exhaustion.

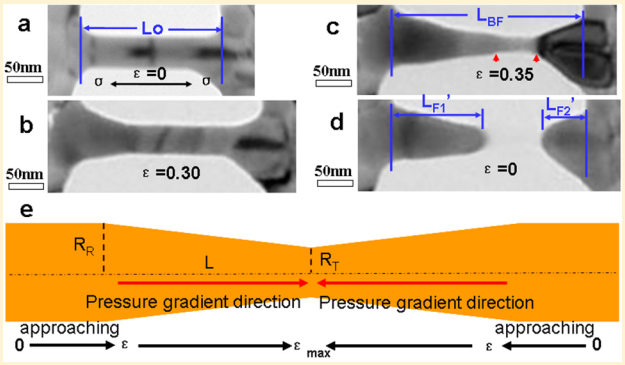

KEYWORDS: *Crystalline-liquid-rubber (CRYS-LIQUE-R), nanowires, large retractable strain, single crystalline Cu, pressure gradient, effective diffusion, in situ TEM*

As a subset of nanostructured materials, the metallic nanowires have emerged as an important structural component in the design of nanorelated materials[1] and devices[2−4] due to their extraordinary properties, especially for the excellent mechanical properties, such as ultrahigh strength[5,6] and ultralarge elasticity[7−10] and superplasticity[11−21] 21 comparing to their bulk counterparts. The details of the elastic-plastic transitions of the metallic nanowires under external stress and strain[12−21] have been clarified. The observed maximum elasticity in metals is in Cu nanowires (NWs) by 7.2%.[22] The ultralarge elasticity of metallic nanowires has also been successfully exploited in composite materials.[23] However, uncertainties have remained, for example, when these huge elastic energies stored in the strained nanowires are released in a short time, like fracture, what will be the consequence? Can the fractured tip be melted or will the fractured tip keep the crystalline features? How large can the retractable strain be? Here, via in situ TEM tensile tests on copper nanowires with an advanced tensile device at a temperature close to room temperature, an astonishing CRYS-LIQUE-R behavior of the fractured single crystalline Cu nanowires was revealed. The retractable strain of the fractured crystalline nanowires approaches over 35%. These abnormal behaviors originate from the fast release of the ultralarge elastic energy of the tensile nanowires. These results are important for nanostructural applications.

High-purity polycrystalline Cu film was prepared by magnetron sputtering method.[22] The film was transferred to a recent developed homemade in situ TEM tensile device.[24] The device was then put in the heating TEM holder. The pulling force was provided by the deformation actuators,[22,25−31] made of sheets with different thermal expansion coefficients. Upon slightly heating (on a 3 mm diameter copper-ring grid) in the TEM heating holder, the plates bend, the two plates were arranged to bend in opposite directions, actuating the pulling of the sample. Crack propagation can give a large space due to

Received: May 19, 2013
Revised: June 21, 2013
Published: July 30, 2013

 © 2013 American Chemical Society dx.doi.org/10.1021/nl401829e | *Nano Lett.* 2013, 13, 3812−3816

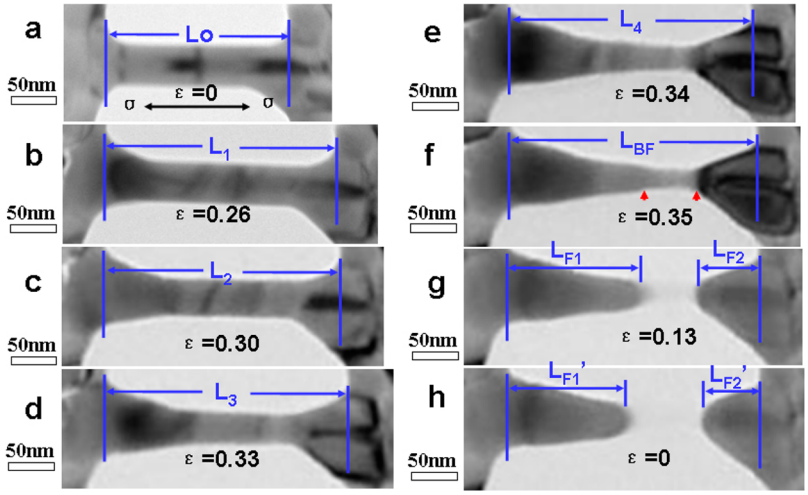

Figure 1. An example of a single crystal Cu NW under uniaxial tensile test with a recoverable strain up to ~35%. (a–f) The continuous tensile process before fracture; (f–h) the dynamic fracture process of the nanowires with a huge recoverable strain up to ~35%.

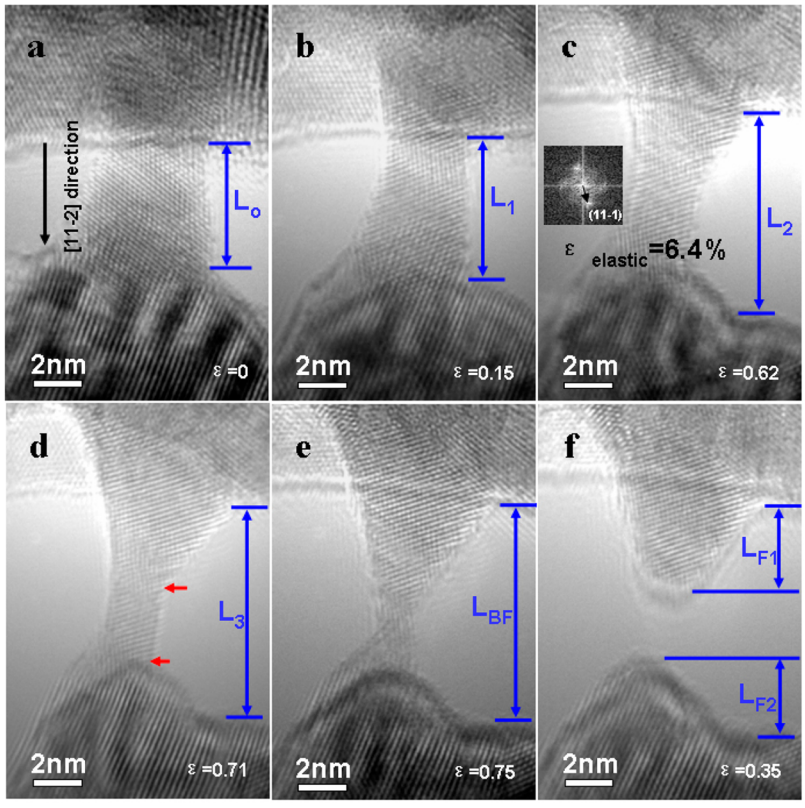

Figure 2. Shows a series of HREM image of a single crystal Cu NW under uniaxial tensile test. L_o–L_{BF} labeled in panels a–e denote the gauge length of the nanowire at different states. L_{F1} and L_{F2} in panel f marked the final length of the nanowire after fracture.

temperature increase that can drive the movement of these two deformation actuators. The bending velocity can be changed according to the experiments via adjusting the heating controller outside of the TEM. During the pulling test, cracks/voids will form and some ligaments will be left and bridged on the cracks/voids; our focus is on these ligaments, which will be taken as single crystal Cu NWs with diameter below 50 nm.

Figure 1 shows a tensile test of a single-crystal Cu NW with diameter of ~45 nm. The two blue lines in Figure 1 marked the gauge length used for our subsequent "nanowire tensile" experiment. The loading direction was also labeled by a double-head arrow and "σ" in Figure 1a. The original gauge length was also marked with L_o as shown in Figure 1a. Figure 1a–f shows the continuous tensile process and a high plastic deformation strain of ~35% has been achieved before fracture (see L_{BF} in Figure 1f). With further pulling, fracture occurred in Figure 1g. Figure 1f–h shows the dynamic retracting processes of the fractured tips. Comparing the shape shown in Figure 1f–h, we can find the nanowire retracted with length reduction and diameter expansion simultaneously. As shown in Figure 1h, the sum of the final length of the fractured ends ($L_{F1'}$ + $L_{F2'}$)

dx.doi.org/10.1021/nl401829e | *Nano Lett.* 2013, 13, 3812–3816

between the two blue lines has decreased and equals to the original length (L_o) of the nanowires. This means that a nearly 35% retractable strain has been achieved. After the test, we have confirmed that the loading direction was nearly along its [11$\bar{2}$] direction with the selected area diffraction pattern (SAEDP) of the nanowires (see more details in ref 32). Supporting Information Movie 1 shows the dynamic fracture process; a rubber-like behavior in this fractured metallic nanowire has been demonstrated.

Further, an in situ atomic scale tensile test demonstrated that the fractured nanowires kept its crystalline character during the whole fractured process. Figure 2 shows a series of atomic scale HRTEM images taken during the tensile and fracture process of the tested nanowire. The tested single-crystal Cu nanowire was a diameter less than ~5 nm along [11$\bar{2}$] direction. Figure 2a–f shows the tensile and fracture process. According to the change of (11$\bar{1}$) interplanar spacing as marked by the black arrow in the insert image in Figure 2c, the largest elastic strain can be measured and it was about ~6.4%. Then severe necking occurred at the point marked by a blue arrow in Figure 2d. With strain further increasing, the fracture occurred (Figure 2e,f) and the two tips of the fractured nanowire retracted rapidly. Comparing L_{BF} in Figure 2e with $L_{F1} + L_{F2}$ in Figure 2f, the length of the nanowire shrunk with about ~40% retractable strain. The shape of the nanowire also became shorter and fatter after fracture (compare Figure 2e with Figure 2f) as revealed in Figure 1. As shown in Figure 2e,f, the two fractured nanowire tips kept their single crystalline structure through the whole fracturing process. This directly demonstrated that the no-melting process occurred in this rubber-like behavior of the crystalline nanowire nanofracture process.

The rubber-like retractable strain of the fractured nanowire tips exceeded 35% (~35% in Figure 1 and ~40% in Figure 2), which far exceeds the theoretical elastic strain limits of metallic materials. This huge retractable strain of the fractured crystalline metallic nanowires is, however, similar to a fractured rubber tip. This is an astonishing phenomenon that rarely happens in materials with metallic bonds. We speculate the following aspects may contribute to rubber-like behavior of the fractured nanowires. The first contribution of the rubber-like behavior comes from the release of the ultralarge true elastic strain.[22] As mentioned above and in multiple investigations, for a copper wire with diameter of ~15 nm (the region marked by two red arrows in Figure 1f) its elastic strain limit can be as high as ~6.5% according to our previous study.[22] The measurable maximum elastic strain of nanowires in this study has reached 6.4% (Figure 2c) and is close to the theoretical values of 8%.[33] So, the internal elastic energy stored during the tensile test is very high. Taking Figure 1 as an example, the stored elastic energy can be about 5.6×10^{-15} J. After fracture, due to the release of such high elastic energy, a huge pressure will be loaded to the atoms of the pyramid-shaped tip. A pressure gradient pointing to the reverse direction of tensile stress of the nanowire will be formed. In the meantime, the stored elastic energy will transform to the thermal energy during the retracting process, leading to an obvious temperature increase of the fractured NW tip. The diffusion coefficient of atoms of the fractured tips will thus be enhanced by the pressure gradient and the increase of the temperature (see ref 32).

Taken Figure 1 as an example, the atoms on the largest strain region (the region marked by two red arrows in Figure 1f) still endure a huge pressure that can be estimated ~8.5 GPa (take 6.5% as the maximum elastic strain in Figure 1). After the fracture occurred, such a high pressure (~8.5 GPa) will be loaded to atoms of the fractured tips and the diffusion coefficient will be sharply increased. Figure 3 shows a predigested model. As seen in Figure 3a, a severe necking has happened and the pressure gradient direction has been marked by two red arrows; R_R and R_T denote the radii of the root and the tip of the plastic region, and there will be a high pressure gradient due to the cross-sectional area decrease along this direction. The elastic strain also has a gradient that changed gradually from zero to ε_{max}. If we take two adjacent layers as an example, P_2 and P_1 denote the pressure loaded to these two atom layers, and then we will have an effective diffusion coefficient that will be calculated from the following formula:[34]

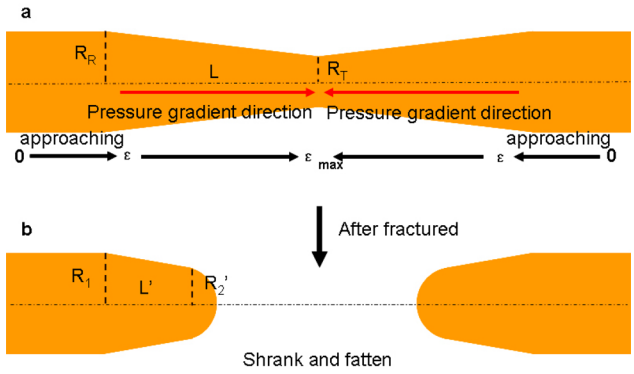

Figure 3. (a,b) A simple sketch map of the rubber-like behavior of the fractured single crystalline Cu nanowire tips.

$$D_{eff} = D\left(1 + \frac{P_2 - P_1}{P_1}\right)e^{-Z/L_C} \quad (1)$$

where, L_C is the effective decay length. Z is the length along Z direction, which is opposite to the pressure gradient direction. From the formula shown above, we can find if there is a difference in the pressure loaded to these two atom layers, an effective diffusion will be triggered. Taking into account the integrated effect, the top layer will diffuse to the crystal with the largest diffusion length, L_{max}, which can be calculated using the following equation:

$$L_{max} = \sqrt{4D_{eff-max}t} \quad (2)$$

Here, we should also consider the influence come from the temperature increases induced by the TEM holder. Then

$$D_{eff} = D_0 e^{-E_a/RT}\left(1 + \frac{P_2 - P_1}{P_1}\right)e^{-Z/L_C} \quad (3)$$

For copper, $D_0 = 7.8 \times 10^{-5}$ m^2/S; the activation energy E_a is ~211 kJ/mol;[35] P_2 is the maximum pressure, which is about 8.5 GPa in the current case; P_1 is the internal pressure in our TEM system, which is about 0.1×10^{-5} Pa. Then, we have $D_{eff\text{-}max} \sim 2 \times 10^{-17}$ m^2/S, the maximum effective diffusivity estimated though eq 3. According to Supporting Information Movie 1, the whole diffusion process continued ~0.5 S and thus the maximum diffusion length is about 6.3 nm, that is, atoms on the fractured tips with a huge pressure (~8.5 GPa) loaded on it will travel about 6.3 nm inner the wire during the instant process of fracture. The travel length will have a gradient and a maximum length will occurred on the "tip" atoms. This phenomena is just

dx.doi.org/10.1021/nl401829e | Nano Lett. 2013, 13, 3812–3816

like a punch to the nanowires, then a fatter and shorter shape in Figure 3b will be formed. As seen in Figure 1f–h, there is a large retractable strain of ~35%. If we take the most severe deformation region as an typical example (see the region marked by two red arrows in Figure 1f, the length is about 45 nm) the retractable strain induced by diffusion will be up to 14% when taking the maximum diffusion length as 6.3 nm. With the elastic strain added (as mentioned above, ~6.5%), the minimum and measurable total retractable strain is over 20%.

On the other hand, the general diffusion process can be characterized by a barrier with activation energy E_a, where E_a is the energy required for an atom to jump from one site to the next. The diffusivity can be written as[36,37]

$$D = D_o \exp\left(-\frac{E_a}{RT}\right) \quad (4)$$

Where, D_o denotes the pre-exponential factor also called the frequency factor, and E_a is the activation energy. In this test, in order to load force to the nanowires an extra temperature increase ~100 K has been introduced to drive the two deformation actuators as mentioned above, so when the fracture happened, the temperature of the system is about 373 K, as shown in eq 4, diffusivity will be slightly increased.[32] Furthermore, after the fracture the huge elastic stored energy will transform to be concomitant thermal energy that can lead the system temperature to further increase. It is estimated that the concomitant increased temperature of the fractured tips can be as close as 0.6 Tm (Tm is the melting point for copper,[38] see more details in refs 32 and 39), that is, after the release of such huge elastic energy, a general diffusion process will be highly active that will induce further retracting process. This will add additional retracting strain. The highly activated diffusion process is liquid-like but in crystalline solids.

Finally, through molecular dynamic simulations, a dislocation nucleation and exhaustion process trigged by the very high reverse stress was revealed. Figure 4 shows a retract process of the nanowire and Figure 4a shows the initial state of the nanowire with a preset elastic strain of ~5.5%. Then the nanowire was released. An elastic recovering process can be monitored. As seen in Figure 4b, after the release of the elastic strain, partial dislocations appeared due to the high reverse stress. Then partial dislocations will be exhausted and no dislocation left in the nanowire (Figure 4c,d). This is consistent well with the observation under HREM (Figure 2e). Dislocation nucleation and exhaustion dominated the process. Comparing Figure 4 panels a and d, the nanowire become shorter and fatter, which is similar to the phenomena revealed in Figures 1 and 2. For the very short-lived simulation time and small pressure gradient, the diffusion is not so obvious compared to our experimental results.

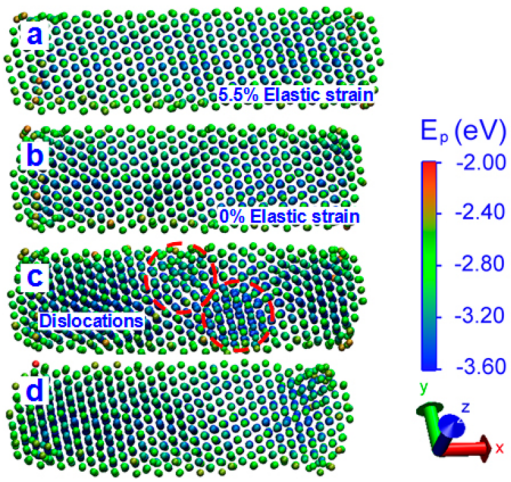

Figure 4. MD simulation result shows the retraction process. (a) The state of the nanowire with a preset elastic strain of ~5.5%; (b) The instant morphology of the nanowire after the release of the elastic strain with 0 strain; (c,d) The continuous deformation process after fracture.

Via in situ TEM tensile tests of copper nanowires with an advanced tensile device, a crystalline liquid and rubber-like behavior of single crystalline Cu nanowires' fractured tips has been revealed. The retractable strain of the fractured nanowires approached over 35%. This astonishing CRYS-LIQUE-R fracture behavior originates from an instant release of the stored ultralarge elastic energy. Such huge elastic energy release induced three main processes: the first one is the recovering of true elastic strain, the second one is huge atom diffusion process induced by pressure gradient; and the third is the enhanced diffusion process induced by the temperature increase. The CRYS-LIQUE-R behavior of the fractured tip includes both of elasticity and plasticity activities. A unique CRYS-LIQUE-R behavior of nanomaterials was thus revealed. This CRYS-LIQUE-R behavior is obviously interesting for applications, such as those in micro- or nanoelectromechanical systems (MEMS or NEMS) and flexible devices.

■ ASSOCIATED CONTENT

Supporting Information

Additonal information and video. This material is available free of charge via the Internet at http://pubs.acs.org.

■ AUTHOR INFORMATION

Corresponding Author

*E-mail: (X.H.) xdhan@bjut.edu.cn; (S.Z.) zhangs9@rpi.edu; (Z.Z.) zezhang@zju.edu.cn.

Notes

The authors declare no competing financial interest.

■ ACKNOWLEDGMENTS

This work was supported by China National Nature Science Foundation (11234011, 11127404) and the National 973 Program of China (2009CB623700).

■ REFERENCES

(1) Cui, Y.; Lieber, C. M. *Science* **2001**, *291*, 851–853.
(2) Lieber, C. M. *MRS Bull.* **2003**, *28*, 486–491.
(3) Huang, Y.; Duan, X.; Cui, Y.; Lauhon, L.; Lieber, C. M. *Science* **2001**, *294*, 1313–1317.
(4) Tian, B.; Zhang, X.; Kempa, T. J.; Fang, Y.; Yu, N.; Yu, G.; Huang, J.; Lieber, C. M. *Nature* **2007**, *449*, 885–890.
(5) Kovtyukhova, N. I.; Mallouk, T. E. *Chem.—Eur. J.* **2002**, *8*, 4354–4363.
(6) Kondo, Y.; Takayanagi, K. *Phys. Rev. Lett.* **1977**, *79*, 3455–3458.
(7) Mehrez, H.; Ciraci, S. *Phys. Rev. B.* **1997**, *56*, 12632–12642.
(8) Kang, J. W.; Hwang, H. J. *Nanotechnology* **2001**, *12*, 295–300.
(9) da Silva, E. Z.; da Silva, A. J. R.; Fazzio, A. *Phys. Rev. Lett.* **2001**, *87*, 256102:1–4.
(10) Branício, P. S.; Rino, J. P. *Phys. Rev. B.* **2000**, *62*, 16950–16955.
(11) Miller, R. E.; Shenoy, V. B. *Nanotechnology* **2000**, *11*, 139–147.
(12) Brenner, S. S. *J. Appl. Phys.* **1956**, *27*, 1484–1491.
(13) Herring, C.; Galt, J. K. *Phys. Rev.* **1952**, *85*, 1060–1061.

(14) Richter, G.; Hillerich, K.; Gianola, D. S.; Monig, R.; Kraft, O.; Volkert, C. A. *Nano Lett.* **2009**, *9*, 3048−3052.
(15) Ganesan, Y.; Lu, Y.; Peng, C.; Lu, H.; Ballarini, R.; Lou, J. *J. Microelectromech. Syst.* **2010**, *19* (3), 675−682.
(16) Zhu, Y.; Espinosa, H. D. *Proc. Natl. Acad. Sci. U.S.A.* **2005**, *102*, 14503−14508.
(17) Zhang, D. F.; Breguet, J. M.; Clave, R.; Philippe, L.; Utke, I.; Michler, J. *Nanotechnology* **2009**, *20*, 365706:1−7.
(18) Wu, B.; Heidelberg, A.; Boland, A. J. *Nat. Mater.* **2005**, *4*, 525−529.
(19) Bei, H.; Shim, S.; Pharr, G. M.; George, E. P. *Acta. Mater.* **2008**, *56*, 4762−4770. Lowry, M. B.; Kiener, D.; LeBlanc, M. M.; Chisholm, C.; Florando, J. N.; Morris, J. W., Jr; Minor, A. M. *Acta. Mater* **2010**, *58*, 5160−5167.
(20) Sriram, V.; Yang, J. M.; Ye, J.; Minor, A. M. *Micro. Eng.* **2010**, *87*, 2046−2049.
(21) Zheng, H.; Cao, Ajing.; Weinberger, C. R.; Huang, J. Y.; Du, K.; Wang, J. B.; Ma, Y. Y.; Xia, Y. N.; Mao, S. X. *Nat. Commun.* **2010**, *1*, 144:1−7.
(22) Yue, Y. H.; Liu, P.; Zhang, Z.; Han, X. D.; Ma, E. *Nano Lett.* **2011**, *11*, 3151−3155.
(23) Hao, S. J.; Cui, L. S.; Jiang, D. Q.; Han, X. D.; et al. *Science* **2013**, *339*, 1191−1194.
(24) (a) Han, X. D.; Zhang, Y. F.; Zhang, Z. Chinese Patents No. 200610169839.3 and No. 200610144031.x. (b) Han, X. D.; Yue, Y. H.; Zheng, K.; Zhang, Y. F.; Zhang, Z. Chinese Patents No. 200810056836.8.
(25) Wang, L. H.; Han, X. D.; Liu, P.; Yue, Y. H.; et al. *Phys. Rev. Lett.* **2010**, *105*, 135501:1−4.
(26) Liu, P.; Mao, S. C.; Wang, L. H.; Han, X. D.; et al. *Scr. Mater.* **2010**, *64*, 343−346.
(27) Wang, L. H.; Zhang, Z.; Ma, E.; Han, X. D. *Appl. Phys. Lett.* **2011**, *98*, 051905:1−3.
(28) Deng, Q. S.; Cheng, Y. Q.; Yue, Y. H.; et al. *Acta Mater.* **2011**, *59*, 6511−6518.
(29) Zhang, Y. F.; Han, X. D.; Zheng, K.; Zhang, Z.; et al. *Adv. Funct. Mater.* **2007**, *17*, 3435−3440.
(30) Yue, Y. H.; Liu, P.; Deng, Q. S.; Ma, E.; Zhang, Z.; Han, X. D. *Nano Lett.* **2012**, *12*, 4045−4049.
(31) Yue, Y. H.; Wang, L. H.; Zhang, Z.; Han, X. D. *Chin. Phys. Lett.* **2012**, *29*, 066201:1−4.
(32) Supporting Information.
(33) Cao, A.; Wei, Y. G.; Ma, E. *Phys. Rev. B.* **2008**, *77*, 195429:1−5.
(34) Bal, J. K.; Hazra, S. *Phy. Rev. B.* **2009**, *79*, 155405:1−6.
(35) Brandes, E. A.; Brook, G. B. *Smithells Metals Reference Book*, 7th ed.; Butterworth-Heinemann, Oxford, 1992.
(36) Dyakonov, M. I. *Spin Physics in Semiconductors*; Springer Series in Solid-State Sciences; Springer: New York, 2008.
(37) See Jones, S. W. *Diffusion in Silicon*; www.icknowledge.com (accessed March 6, 2013).
(38) Gladkich, N. T.; Niedermayer, R.; Spiegel, K. *Phys. Status Solidi* **1966**, *15*, 181−192.
(39) Liu, Y. H.; Liu, C. T.; Wang, W. H.; Inoue, A.; Sakurai, T.; Chen, M. W. *Phys. Rev. Lett.* **2009**, *103*, 065504:1−4.